Plasmon Resonances and Their Quality Factors in a Finite Linear Chain of Coupled Metal Wires

Nadiia P. Stognii, *Student Member, IEEE*, and Nataliya K. Sakhnenko, *Senior Member, IEEE*

***Abstract*—This paper presents a straightforward analysis of the plasmonic properties of metal wires arranged in a linear chain of a finite length. For this we solve eigenvalue problem in form of matrix equations that allow thorough investigation of plasmonic modes with different field distributions. Our modeling provides results in terms of eigen oscillating frequencies and quality factors with controllable accuracy. It has revealed the possibility of quality factor dramatic enhancement for certain plasmonic modes by adjusting the separation distances and increasing the number of wires in a chain.**

***Index Terms*—Eigenvalues, nanowires, plasmons.**

I. Introduction

METALLIC nanostructures are the subject of immense interest in recent years due to the possibility of a strong light localization beyond the diffraction limit via the excitation of surface plasmons (SPs) [1], [2]. Various elements such as plasmonic waveguides [3], [4], subwavelength resonators [5], [6] and optical nanoantennas [7]–[9] have been studied recently. SPs have been explored for their potential in a single molecule detection [10], [11], biomolecular interaction studies [12], early stage cancer detection [13], [14], transmissions through the subwavelength apertures [15], [16], subwavelength imaging [17], etc.

Plasmonic structures of different shapes (nanowires, nanorods, nanospheres, and nanoshells) can be produced by various fabrication techniques. The silver nanowire structure is a candidate for key components in future ultracompact photonic devices [18]. It can be considered as a plasmon biosensor to monitor tiny biomolecular interactions [19] and as a novel modulator to control the intensity of the transmitted surface plasmon polaritons through a nanowire array [20]. Possible future nanophotonic technologies demand devices that can generate stimulated emission through the excitation of the SPs (spaser-based nanolaser). However, it is challenging problem due to the extremely strong absorption losses in metal at optical frequencies. The suggestion to compensate the losses by an optical gain using dye molecules in presence of metal nanoparticles [21] or using nanoparticles with gold core and dye-doped silica shell [22] has been tested in experiments recently. For these applications an accurate modeling that provides a valuable insight into fundamental phenomena is of great importance.

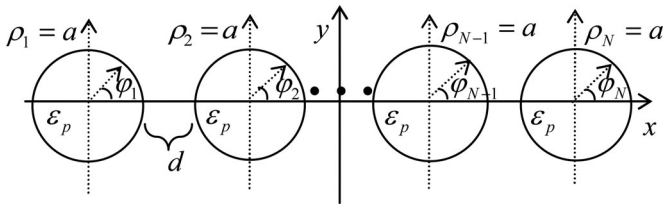

Fig. 1. Schematic diagram of the structure.

The plasmon resonances of nanoparticles with dimensions down to 2 nm can be investigated using classical Maxwell's theory [23], and their optical properties are characterized by their frequency dispersive complex permittivity. The resonance plasmon frequencies strongly depend on the particle size and shape. The plasmonic modes of coupled nanoobjects can be considered as symmetric and antisymmetric combinations of SPs of isolated objects with different frequencies and field portraits [24]–[28].

The plasmonic properties of nanowires and nanoparticles have recently been investigated using a variety of methods [4], [23]–[26], [32]. However, there is a lack of investigations in terms of quality Q factors of SPs, though these characteristics are of crucial importance in problems associated with spectral resolution of sensors, stimulated emission enhancement, etc. Many authors find SPs investigating resonance peaks in scattering cross section (SCS). This study cannot be considered as a complete one, because in this way only "bright" plasmons can be seen, "dark" plasmons that do not couple efficiently to incident wave cannot be discovered in such a description.

In this paper, we develop nonquasistatical expressions for the eigenvalues of SPs using the extension of the Drude formula to complex values that includes finding of eigenfrequencies and Q. Using this approach, all possible SPs can be found and investigated, including "dark" and multipole ones.

II. Mathematical Background

It is known that SPs can exist on a metal wire that can be considered as a plasma infinite-long cylinder (column) in the optical region. In this paper, we study the SP resonances in an isolated infinite-long wire and in a finite linear chain of coupled wires, surrounded by vacuum. The radius of each wire is a, the separation distance between them is d (air gap between the wires or interwires spacing), the time dependence $e^{i\omega t}$ is implied. Fig. 1 represents a schematic diagram of the structure. Cylinders with ordinary nonmagnetic metal are characterized by

Manuscript received August 1, 2012; revised January 1, 2013; accepted January 25, 2013. The work of the author N. Stognii was supported by the German Academic Exchange Service (DAAD). The work of the author N. K. Sakhnenko was supported by the European Science Foundation Research Networking Programme PLASMON-BIONANOSENSE.

The authors are with the Department of High Mathematics, Kharkiv National University of Radio Electronics, Kharkiv 61166, Ukraine (e-mail: nstognii@gmail.com; n_sakhnenko@yahoo.com).

Digital Object Identifier 10.1109/JSTQE.2013.2244561

a negative permittivity $\varepsilon < 0$ and support only TE polarized SPs. The frequency dependent metal's permittivity ε_p is described by the Drude model

$$\varepsilon_p = 1 - \omega_p^2/(\omega(\omega - i\gamma)) \tag{1}$$

where ω_p represents the plasma frequency and γ is the material absorption. We will assume that ω can be complex valued.

In this paper, the Maxwell equations are the underlying equations of the analysis

$$\text{rot}\,\vec{E} = -i\omega\mu_0\vec{H} \tag{2}$$

$$\text{rot}\,\vec{H} = i\omega\varepsilon_0\varepsilon\vec{E} \tag{3}$$

where $\vec{E}$ and $\vec{H}$ represent the vectors of electric and magnetic fields, ε_0 and μ_0 are the electric and magnetic constants, ε should be replaced by ε_p for inner points of wires, otherwise $\varepsilon = 1$.

To characterize the fields we introduce N cylindrical system of coordinates associated with each wire (see Fig. 1) and the global Cartesian (x, y, z) system centered at the midpoint of the structure. It is assumed that the columns are oriented along the axis *Oz*. *TE*-polarized fields are considered with H_z, E_φ, E_ρ nonzero components.

Maxwell's equations (2), (3) lead to the Helmholtz equation for the z-component of the magnetic field, which is denoted below as H

$$\Delta H + k^2 H = 0 \tag{4}$$

where $\Delta = \partial^2_{\rho\rho} + 1/\rho\partial_\rho + 1/\rho^2\partial^2_{\varphi\varphi}$ is the Laplace operator, $k = \omega/c$ represents the wave number of vacuum, c is the light velocity in vacuum, for inner points of each wire $k = k_p$, and $k_p = n_p\omega/c$ is the wave number of plasma $n_p = \sqrt{\varepsilon_p(\omega)}$.

A. Isolated Infinite-long Metal Wire

We first investigate the SPs on isolated wire excited by a plane wave $H = e^{-ik(x\cos\alpha + y\sin\alpha)}$, here α is the angle between the direction of propagation of a plane wave and the positive direction of the x-axis (it is a z-component of the incident field, the normalizing factor is omitted). The transmitted and the scattered magnetic fields, respectively, are expanded as

$$H(\rho,\varphi) = \sum_{s=-\infty}^{+\infty} A_s J_s(k_p\rho)e^{is\varphi}, \quad \rho < a \tag{5}$$

$$H(\rho,\varphi) = \sum_{s=-\infty}^{+\infty} \bar{A}_s H_s^{(2)}(k\rho)e^{is\varphi}, \quad \rho > a \tag{6}$$

where A_s and $\bar{A}_s$ are unknown expansion coefficients. It should be noted that outside the wire the total field is the sum of incident plane wave and scattered field. The incident plane wave can be represented in the form of a series of the Bessel functions

$$e^{-ik(x\cos\alpha + y\sin\alpha)} = e^{-i\rho\cos(\varphi-\alpha)} = \sum_{s=-\infty}^{\infty} (-i)^s J_s(k\rho)e^{is(\varphi-\alpha)}. \tag{7}$$

The boundary conditions, that require the tangential components of the total electric and magnetic fields to be continuous at the surface, for this polarization can be written as follows:

$$H(\rho = a+0) = H(\rho = a-0) \tag{8}$$

$$\partial H/\partial\rho(\rho = a+0) = \varepsilon_p \cdot \partial H/\partial\rho(\rho = a-0). \tag{9}$$

Unknown coefficients are found by virtue of the substitution of (5), (6) and (7) into (8) and (9)

$$A_s = -(-i)^s e^{-is\alpha} n_p 2i/(\pi a)\cdot 1/F_s \tag{10}$$

$$\bar{A}_s = (-i)^s e^{-is\alpha}\cdot V_s/F_s \tag{11}$$

where

$$F_s = H_s^{(2)'}(ka)J_s(k_p a) - 1/n_p H_s^{(2)}(ka)J_s'(k_p a) \tag{12}$$

$$V_s = J_s'(ka)J_s(k_p a) - 1/n_p J_s(ka)J_s'(k_p a) \tag{13}$$

where the prime denotes the derivative with respect to the function's entire argument.

The plasmonic modes of the metal wire (the field in the absence of the incident field) can be written as

$$H = \begin{cases} AJ_s(k_p\rho)e^{is\varphi}, & \rho < a \\ \bar{A}H_s^{(2)}(k\rho)e^{is\varphi}, & \rho > a. \end{cases} \tag{14}$$

Similarly from the boundary conditions (8)–(9), one can obtain

$$A = \bar{A}H_s^{(2)}(ka)/J_s(k_p a) \tag{15}$$

and dispersion relation for eigenfrequencies of the wire

$$F_s = 0 \tag{16}$$

where F_s is given by (12). Equation (16) determines the eigenfrequencies of the isolated wire. We are interested in plasmonic modes, so we have to examine only the region $\omega < \omega_p$. In this interval (16) has no solution for the case $s = 0$, but for each integer positive s it has a unique plasmonic solution. SP with $s = 1$ can be considered as dipole SP, with $s = 2,\ 3, ...$ as multipole SPs.

B. Finite Linear Chain of Coupled Infinite-long Wires

The approach aforementioned can be extended to the case of N coupled metal wires arranged in a linear chain (see Fig. 1). For this, field representations which are similar to (5)–(6), have to be written for each wire

$$H(\rho_m,\varphi_m) = \sum_{s=-\infty}^{+\infty} A_s^m J_s(k_p\rho_m)e^{is\varphi_m}, \quad m = (1, ..., N) \tag{17}$$

$$H(\rho,\varphi) = \sum_{m=1}^{N}\sum_{s=-\infty}^{+\infty} \bar{A}_s^m H_s^{(2)}(k\rho_m)e^{is\varphi_m}. \tag{18}$$

Here, (17) presents internal field for each particular wire, while (18) characterizes external field, global polar coordinates (ρ, φ) are associated with the (x, y) Cartesian system. Unknown coefficients are found from the boundary conditions (8), (9) applied on each surface. Using the addition theorem for the Bessel functions we arrive at an infinite system of algebraic equations that can be truncated in order to provide a controlled numerical precision. The solution of the plane wave scattering problem on

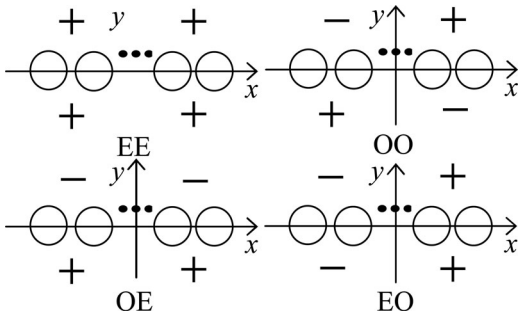

Fig. 2. Four classes of symmetry of the field: EE (x- even, y- even), OO (x- odd, y- odd), OE (x- odd, y- even), EO (x- even, y- odd).

a linear chain of silver nanowires is derived in [29]. In this paper, we concentrate on deriving the formulas for eigenfrequencies. For this we solve eigenvalue problem with zero incident field. Generally, the plasmonic eigenfrequencies of the linear chain are zeros of the N-block matrix determinant equation. With growing of N the solution of the equation becomes more time-consuming. However, the problem can be simplified using the following observations. The structure under consideration has two axes of symmetry, which causes four families of excited plasmons. They can be classified as EE SPs with field distributions symmetrical with respect to x- and y-axes, EO SPs with field distributions symmetrical (even) with respect to x-axis and antisymmetrical (odd) with respect to y-axis), similarly, OE (x-odd; y -even), OO (x-odd; y-odd). Here, we follow classification proposed in [30], [31] for eigenmodes in thin disks photonic molecules.

Fig. 2 shows the classification scheme of possible SP symmetry classes in a finite linear chain. For each symmetry class, the eigenfrequency equation can be simplified and written in the following form:

EE (x-even, y-even)

$$x_m^{(p)} + J_m(ka)\sum_{j=1}^{N/2}\sum_{s=0}^{\infty}\mu_s x_s^{(j)} U_s W_{ms}^{(p,j)} + \\ + 2J_m(ka)\sum_{s=0}^{\infty}\mu_s x_{2s}^{(N+1)/2} U_{2s} W_{m,2s}^{(p,(N+1)/2)} = 0 \quad (19)$$

OE (x-odd; y-even)

$$x_m^{(p)} - J_m(ka)\sum_{j=1}^{N/2}\sum_{s=1}^{\infty} x_s^{(j)} U_s W_{ms}^{(p,j)} + \\ + 2J_m(ka)\sum_{s=1}^{\infty} x_{2s}^{(N+1)/2} U_{2s} W_{m,2s}^{(p,(N+1)/2)} = 0 \quad (20)$$

EO (x-even; y-odd)

$$x_m^{(p)} - J_m(ka)\sum_{j=1}^{N/2}\sum_{s=0}^{\infty}\mu_s x_s^{(j)} U_s W_{ms}^{(p,j)} + \\ + 2J_m(ka)\sum_{s=0}^{\infty}\mu_s x_{2s}^{(N+1)/2} U_{2s} W_{m,2s}^{(p,(N+1)/2)} = 0 \quad (21)$$

OO (x-odd; y-odd)

$$x_m^{(p)} + J_m(ka)\sum_{j=1}^{N/2}\sum_{s=1}^{\infty} x_s^{(j)} U_s W_{ms}^{(p,j)} \\ + 2J_m(ka)\sum_{s=1}^{\infty} x_{2s}^{(N+1)/2} U_{2s} W_{m,2s}^{(p,(N+1)/2)} = 0 \quad (22)$$

where $m = (1, ...N)$, $p = (1, ...N/2)$ if N is even and $p = (1, ...(N+1)/2)$ if N is odd

$$x_m^{(p)} = A_m^{(p)} F_m J_m(ka)$$

$$U_{ms}^{(p,j)} = \frac{V_s}{F_s J_s(ka)}$$

$$W_{ms}^{(p,j)} = \begin{cases} \pm H_{m+s}^{(2)}((N-j)kh) \pm (-1)^s \\ \qquad H_{m-s}^{(2)}((N-j)kh), \quad p = j \\ H_{m-s}^{(2)}((j-p)kh) \pm (-1)^s H_{m+s}^{(2)}((j-p)kh) \\ +(-1)^s H_{m-s}^{(2)}((N-j)kh) \\ \qquad \pm H_{m+s}^{(2)}((N-j)kh), \quad p \neq j \end{cases}$$

$$W_{ms}^{(p,(N+1)/2)} = H_{m-2s}^{(2)}(((N+1)/2-p)kh) \\ \pm H_{m+2s}^{(2)}(((N+1)/2-p)kh)$$

$$h = 2a + d.$$

In $W_{ms}^{(p,j)}$ we take the sign $+$ for x-even SPs and $-$ for x-odd SPs. We have to stress that last terms in (19)–(22) appear only for odd number of columns in a chain.

Finding the eigenvalues reduces to the computation of zeros of the derived matrix equations determinants (19)–(22). These systems are the Fredholm second kind matrix equations. They can be truncated so that approximate solution will converge to exact solutions with increasing of the truncation number. The truncation number is determined by the wire radii the distance between them, and the desired accuracy. For accurate description of the fields, higher order multipole SPs should be taken into account for closely spaced wires. In this study, the truncation number 20 has been used to provide the 10^{-4} accuracy.

For distant wires due to decaying character of the Hankel functions the influence of the series terms become negligibly small. The derived equations can be viewed as characteristic equations for SP of isolated wire (16).

We have to mention that all eigenfrequencies are complex $\omega = \omega' + i\omega''$, where $\omega'' > 0$ represents damping and ω' is associated with the eigen oscillation frequencies. Q of plasmons can be evaluated through the formula $Q = \omega'/2\omega''$.

III. Results and Discussion

A. Plasmon Resonances of an Individual Metal Wire

For further calculations we will use the normalized parameter $w_p = \omega_p a c^{-1}$ that we will call the size parameter. Fig. 3 shows the spatial near-field portraits of the SPs for $s = 1,\ 2,\ 3$ ($w_p = 0.5$).

Fig. 4 plots the SCS obtained from (5), (6) in far-field limit versus normalized frequency (ka) for different values of

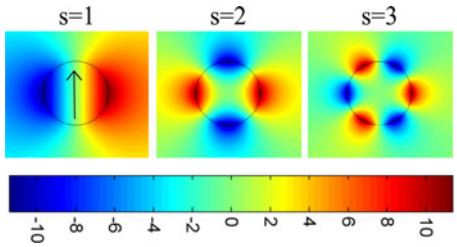

Fig. 3. Near-field distributions ($z-$ coordinate of the magnetic field) of SP for different number of angular field variations ($w_p = 0.5$).

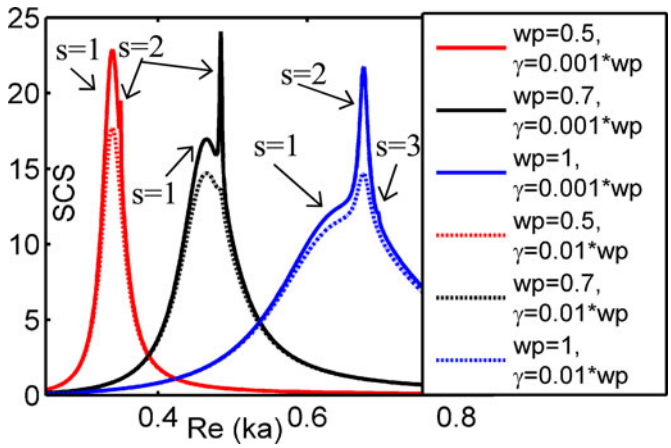

Fig. 4. SCS of isolated metal wire versus normalized frequency (ka) for different values of the size parameter w_p.

w_p. For the value of $w_p = 0.5$ (optically thin wire), we can see only one peak for $\gamma = 10^{-2} w_p$ associated with excited dipole plasmon. Additional sharp peak is observable in the spectrum for smaller value of losses $\gamma = 10^{-3} w_p$, it is associated with quadrupole plasmon. We see an additional prominent sharp peak for $w_p = 0.7$ if $\gamma = 10^{-3} w_p$ that corresponds to the quadrupole plasmon. For optically thick wire $(w_p = 1)$, maximum amplitude is associated with quadrupole SP. The normalized value of $w_p = 0.5$ approximately corresponds to the silver nanowire of 28.3 nm radius, $w_p = 0.7$ and $w_p = 1$ correspond to the 39.1 nm and 56.9 nm, respectively. Fig. 5(a) illustrates the value of the real part of SP normalized eigenfrequency $(\mathrm{Re}(ka) = \omega' a/c, \quad \omega'$ is the real part of eigenfrequency that is the solution of the equation (16)) versus the number of angular field variations (s) for the same values of the size parameters w_p as in Fig. 4. Fig. 5(b) plots Q of corresponding SPs. The dispersion (16) has formal solution for arbitrary number of angular field variations; different solutions for these values of w_p are observable only for a few SPs (dipole and quadrupole ones).

The SPs eigenvalues crowding is seen with growing of s (e.g. for $w_p = 1$ and $\gamma = 10^{-3} w_p$ dipole plasmon normalized eigenfrequency is $ka = 0.63 + 0.1i$, for quadrupole SP $ka = 0.6755 + 0.0068i$, with growing of s eigenfrequencies tend to the approximate value of $ka = 0.7 + 0.0005i$); however, in the spectrum (Fig. 4) only a dipole and quadrupole SPs are seen.

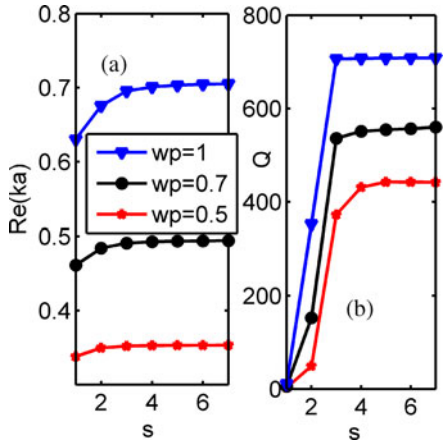

Fig. 5. (a) Dependence of the eigenfrequency on the number of angular field variations for different values of the w_p and (b) dependence of the Q-factor on the number of angular field variations for isolated plasma cylinder $(\gamma = w_p \cdot 5.10^{-3})$.

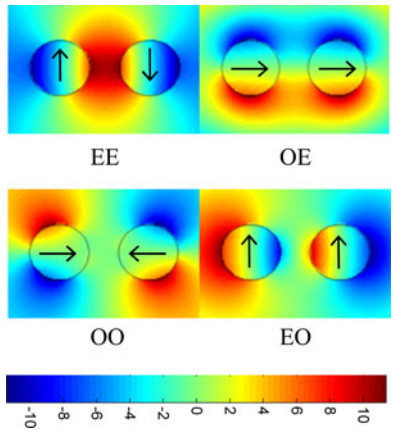

Fig. 6. Near-field distributions (z- coordinate of the magnetic field) of different SPs of two coupled metal wires ($w_p = 0.5$).

B. SPs of Two Coupled Wires

The SPs in dimmers have been extensively studied [23]–[25]. Here, we provide some additional comments in terms of eigenfrequencies and Q. Fig. 6 shows the near-field distributions (17), (18) of EE, EO, OE, OO dipole SPs (19)–(22) of two metal wires that are symmetric and asymmetric combinations of SPs of individual wire. The orientation of their dipole moments is shown in the figures. Dipole EE SP can be viewed as transverse opposite-phase plasmon. Dipole EO SP is transversal in-phase one, OE and OO are longitudinal SPs in-phase and opposite-phase, respectively.

Figs. 7 and 8 demonstrate the real values of the eigenfrequencies and Q for the dipole $(s = 1)$ and quadrupole $(s = 2)$ SPs for two coupled metal wires. Black dashed line plots data for an individual wire. It is clearly seen (see Fig. 7) that for distant wires eigenfrequencies are nearly identical for all four symmetry classes. As separation distance d becomes smaller, the frequency shift of the coupled SPs becomes much stronger.

Fig. 8 represents Q of coupled SP modes for dipole plasmon of optically thin wire $(w_p = 0.5)$ and quadrupole plasmon of thick wire $(w_p = 1)$. Dramatical enhancement of Q is observable

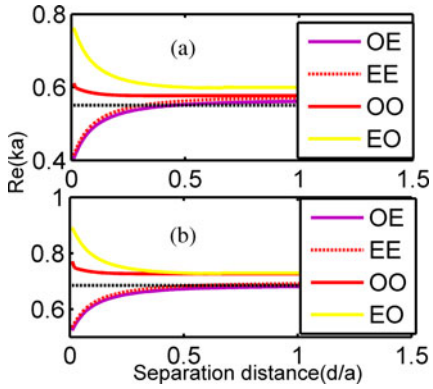

Fig. 7. Dependence of the normalized frequency on the normalized separation distance between two coupled wires for different SPs ($w_p = 1, \gamma = w_p \cdot 10^{-3}$): (a) $s = 1$; (b) $s = 2$.

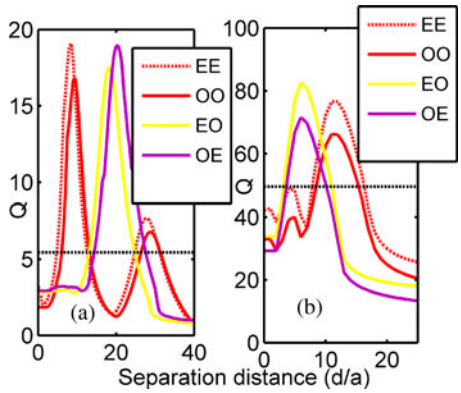

Fig. 8. Q-factor for two coupled metal wires ($\gamma = w_p \cdot 10^{-3}$) for EE, OE, EO, OO plasmons and for isolated wire for: (a) $w_p = 0.5$, s = 1; (b) $w_p = 1$, $s = 2$.

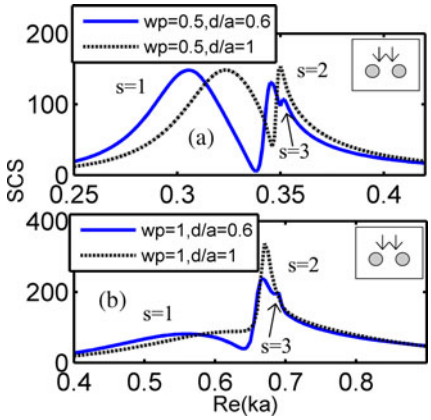

Fig. 9. SCS of a pair of metal wires versus normalized frequency (ka) for different values of the w_p and different values of the normalized separation distance ($\gamma = w_p \cdot 10^{-3}$). Illumination is along the normal to the main axis.

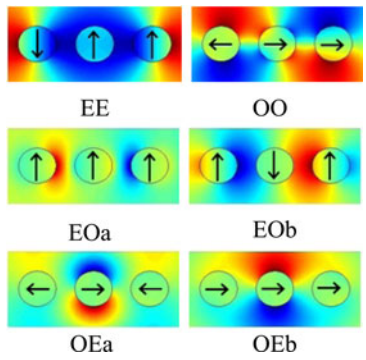

Fig. 10. Near-field distributions ($z-$ coordinate of the magnetic field) of different plasmons of three coupled metal wires.

when $d = 0.97\lambda$ for EE SP, $d = 1.86\lambda$ for EO SP, $d = 1.91\lambda$ for OE SP and $d = 1.025\lambda$ for OO SP (here λ is the wavelength) for thin wire dipole plasmons. Qs of coupled dipole SPs for these values of separation distances are evidently much greater than the Q of individual metal wire SP. For thick wires quadrupole SPs enhancement of Q is observable for following separation distances: $d = 1.43\lambda$ (EE), $d = 0.84\lambda$ (EO), $d = 0.82\lambda$ (OE) and $d = 1.41\lambda$ for OO SP.

In Fig. 9, we report SCS as a function of $\mathrm{Re}(ka)$ for two wires illuminated normally to their main axis. For this illumination direction only OE SPs are excited. It can be easily verified by comparing position of the peak in Fig. 9 and the value of ka in Fig. 7. For "thin" closely spaced wires ($w_p = 0.5, d/a = 0.6$, and $\gamma = w_p \cdot 10^{-3}$) only dipole and quadrupole modes are seen in the spectrum. Further, reduction of the separation distance leads to appearance of additional resonant peak ($s = 3$). With increasing of separation distance the spectrum becomes less complex with main peak at dipole plasmon and finally converges to that of a single wire (see Fig. 4). For thicker wires (lower panel, $w_p = 1$), we observe similar phenomena with main peak at quadrupole plasmon. For the illumination direction parallel to the main axis only EE SPs will be clearly seen in the spectrum, for this reason EE and OE plasmons are referred as "bright," while EO and OO as "dark" ones.

C. SPs of Three Coupled Nanowires

If we add one more metal wire, it would not alter the number of symmetry axes. However, additional solutions can appear in (19)–(22) that characterize bonding and antibonding combinations of the SPs. Thus, if the number of angular field variations is odd, bonding and antibonding SPs appear in EO and OE classes, while systems for EE and OO SPs possess unique solution for given s. However, for even s, we observe reverse situation that means appearance of bonding and antibonding modes in EE and OO classes. Fig. 10 demonstrates the near-field distributions of different dipole plasmons of three coupled wires. The orientation of their dipole moments is schematically shown in the figures. Here, OEb is longitudinal in-phase SP, OEa and OO are longitudinal opposite-phase SPs; EOa is transversal in-phase plasmon; EE and EOb are transversal opposite-phase ones.

Fig. 11 characterize the eigenfrequencies values (their real parts) of the all possible dipole and quadrupole plasmons in a chain of three coupled metal wires. It can be seen that the upward shift in frequency is much faster than downward shift for both dipole and quadrupole modes if wires are brought together. We compare the Q of dipole and quadrupole plasmons in a chain of three metal nanowires in Fig. 12. The growth of Q for certain separation distances is observable. Thus, the positions of Q maxima ($w_p = 0.5$) are: $d \approx 0.64\lambda$ (for EOb and OEb); $d \approx 0.84\lambda$

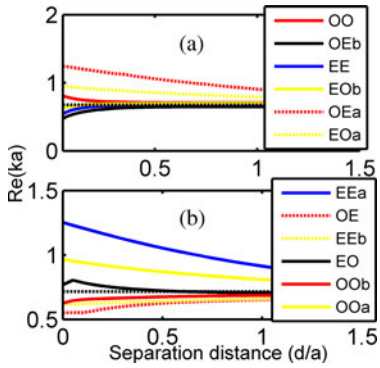

Fig. 11. Normalized frequency versus the normalized separation distance between the three coupled plasma cylinders and for isolated cylinder for different plasmons for $s = 1$ and $s = 2$ ($w_p = 1, \gamma = w_p \cdot 10^{-3}$).

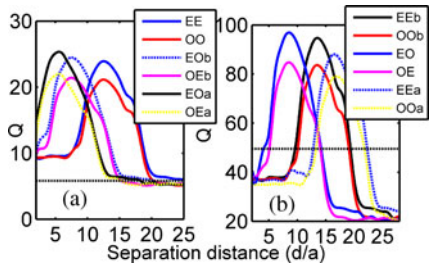

Fig. 12. Q-factor for three coupled plasma cylinders for ($\gamma = w_p \cdot 10^{-3}$) different SPPs for: (a) $w_p = 0.5$, $s = 1$; (b) $w_p = 1$, $s = 2$.

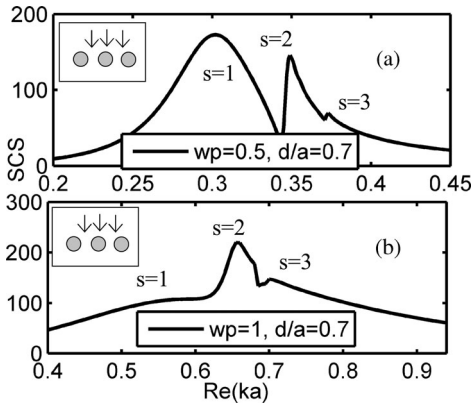

Fig. 13. SCS of three metal wires versus normalized frequency (ka) for different values of the w_p ($\gamma = w_p \cdot 10^{-3}$). Illumination is along the normal to the main axis.

(for EOa and OEa); and $d \approx 1.4\lambda$ (for OO and EE) [see Fig 12(a)]. For greater values of size parameter ($w_p = 1$) the results are presented for quadrupole plasmons [see Fig. 12(b)]. The increasing of Q is observable for $d \approx 0.8\lambda$ (for EO and OE); $d \approx 1.39\lambda$ (for EEa and OOa); and $d \approx 1.73\lambda$ (for EEb and OOb).

Fig. 13 represents the SCS of three metal wires chain with inter wires spacing $d \ll \lambda$. Similarly, to the two wires structure, multiple plasmons are seen in the spectrum. The distant peaks for strongly coupled wires would move closer with decreasing of the separation distance. Illuminating the chain from the top one excites longitudinal in-phase SP (OEb), $s = 2$ peak is associated with OE SP. For the illumination parallel to the main axis transversal opposite-phase EOb dipole plasmon can be excited. For three coupled wires these two dipole plasmons (OEb and EOb) are "bright" ones.

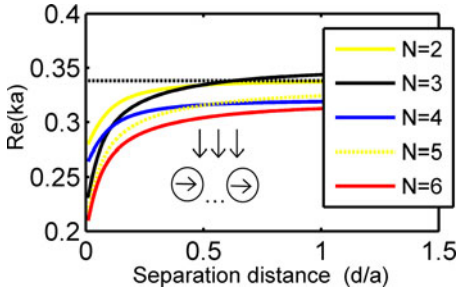

Fig. 14. Normalized frequency versus the normalized separation distance between the coupled metal wires in a chain on N columns for OE plasmon ($s = 1$, w_p =0.5, $\gamma = w_p \cdot 10^{-3}$) and for isolated wire ($s = 1$).

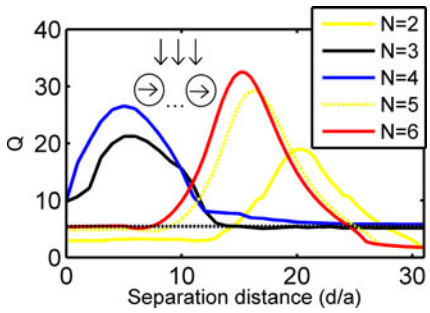

Fig. 15. Q-factor for chain of N coupled plasma cylinders ($s = 1$, $w_p = 0.5$, $y\gamma = w_p \cdot 10^{-3}$) for OE plasmons and for isolated cylinder.

D. P Resonances in a Linear Chain of Coupled Metal Wires

This approach can be extended to an arbitrary finite number of wires in a chain. Thus, in the case of four wires there exist eight SPs for each number of angular field variations, i.e., that each matrix (19)–(22) has two distinct solutions (bonding and antibonding SPs) for given value of s. In general, in the chain of N wires the total number of possible SPs for particular value of s equals to $2N$. In [29] there has been shown that additional resonances (grating-type ones) appear with growing of N (say $N < 50$).

Fig. 14 shows eigenfrequencies of bright dipole SPs for different number of wires in a chain. These SPs can be excited due to the Illumination normal to the major axis. The orientation of the dipole moments is shown in the inset in the figure. These SPs belong to the OE symmetry class. The horizontal line represents eigenfrequency of dipole plasmon of individual metal wire. Extra red shifting of coupled dipole plasmons at small separations is observable.

Enhancement of Q is seen for the same SP modes as aforementioned with appearance of each additional wire. The position of the peak depends on the number of wires; however, the maximum value of Q monotonically grows (see Fig. 15).

IV. Conclusion

We have systematically analyzed the plasmonic properties of a linear chain of metal wires within the Drude model. For this, we have derived matrix equations that allow thorough investigation of SPs. Our modeling provides results in terms of eigen oscillating frequencies and Q. It is shown that SP of coupled wires results from symmetric and antisymmetric combinations of the plasmons of individual wire and strongly depend on interwire separation. It has revealed the possibility of Q dramatic enhancement by virtue of placing the wires at certain distances and increasing the number of wires in a chain.

Acknowledgment

The authors are grateful to Prof. A. I. Nosich for many fruitful discussions.

References

[1] A. Zayats and I. Smolyaninov, "Near-field photonics: Surface plasmon polaritons and localized surface plasmons," *J. Opt. A, Pure Appl. Opt.*, vol. 5, pp. 16–50, 2003.

[2] W. Barnes, A. Dereux, and T. Ebbesen, "Surface plasmon subwavelength optics," *Nature*, vol. 424, pp. 824–830, 2003.

[3] S. Bozhevolnyi, V. Volkov, E. Devaux, J. Laluet, and T. Ebbesen, "Channel plasmon subwavelength waveguide components including interferometers and ring resonators," *Nature*, vol. 440, no. 7083, pp. 508–511, 2006.

[4] Y. Zhao and Y. Hao, "Finite-difference time-domain study of guided modes in nano-plasmonic waveguides," *IEEE Trans. Antennas Propag.*, vol. 55, pp. 3070–3077, 2007.

[5] H. R. Stuart and A. Pidwerbetsky, "Electrically small antenna elements using negative permittivity resonators," *IEEE Trans. Antennas Propag.*, vol. 54, pp. 1644–1653, 2006.

[6] J. li and N. Engheta, "Subwavelength plasmonic cavity resonator on a nanowire with periodic permittivity variation," *Phys. Rev. B*, vol. 74, pp. 1–11, 2006.

[7] P. Muhlschlegel, H. Eisler, O. Martin, B. Hecht, and D. Pohl, "Resonant optical antennas," *Science*, vol. 308, pp. 1607–1609, 2005.

[8] L. Novotny and N. Hulst, "Antennas for light," *Nature Photon.*, vol. 5, pp. 83–90, 2011.

[9] N. Bonod, A. Devilez, B. Rolly, S. Bidault, and B. Stout, "Ultracompact and unidirectional metallic antennas," *Phys. Rev. B*, vol. 82, pp. 1–6, 2010.

[10] K. Kneipp, Y. Wang, H. Kneipp, L. Perelman, I. Itzkan, R. Dasari, and M. Feld, "Single molecule detection using surface-enhanced Raman scattering (SERS)," *Phys. Rev. Lett.*, vol. 78, pp. 1667–1670, 1997.

[11] J. Bahns, A. Imre, V. Vlasko-Vlasov, J. Pearson, J. M. Hiller, L. H. Chen, and U. Welp, "Enhanced Raman scattering from focused surface plasmons," *Appl. Phys. Lett.*, vol. 91, pp. 1–3, 2007.

[12] J. Homola, "Surface plasmon resonance sensors for detection of chemical and biological species," *Chem. Rev.*, vol. 108, no. 2, pp. 462–493, 2008.

[13] S. Mallidi, T. Larson, J. Tam, P. Joshi, A. Karpiouk, K. Sokolov, and S. Emelianov, "Multiwavelength photoacoustic imaging and plamon resonance coupling of gold nanoparticles for selective detection of cancer," *Nano Lett*, vol. 9, no. 8, pp. 2825–2831, 2009.

[14] J. Kah, K. Kho, C. Lee, C. Richard, Sheppard, Z. Shen, K. Soo, and M. Olivo, "Early diagnostics of oral cancer based on the surface plasmon resonance of gold nanoparticles," *Int. J. Nanomedicine*, vol. 2, no. 4, pp. 785–798, 2007.

[15] J. Weiner, "The physics of light transmission through subwavelength apertures and aperture arrays," *Reports Progress Phys.*, vol. 72, pp. 1–19, 2009.

[16] T. Thio, K. Pellerin, R. Linke, H. Lezec, and T. Ebbesen, "Enhanced light transmission through a single subwavelength aperture," *Opt. Lett.*, vol. 26, pp. 1972–1974, 2001.

[17] I. Smolyaninov, J. Elliott, A. Zayats, and C. C. Davis, "Far-field optical microscopy with a nanometer-scale resolution based on the in-plane image magnification by Surface Plasmon Polaritons," *Phys. Rev. Lett.*, vol. 94, pp. 1–4, 2005.

[18] E. Ozbay, "Plasmonics: Merging photonics and electronics at nanoscale dimension," *Science*, vol. 311, pp. 189–193, 2006.

[19] K. Kim, S. J. Yoon, and D. Kim, "Nanowire-based enhancement of localized surface plasmon resonance for highly sensitive detection: A theoretical study," *Opt. Expr.*, vol. 14, no. 25, pp. 12419–12431, 2006.

[20] D. Fedyanin and A. Arsenin, "Transmission of surface plasmon polaritons through a nanowire array: Mechano-optical modulation and motion sensing," *Opt. Expr.*, vol. 18, no. 19, pp. 20115–20124, 2010.

[21] G. Dice, S. Mujumdar, and A. Elezzabi, "Plasmonically enhanced diffusive and subdiffusive metal nanoparticle-dye random laser," *Appl. Phys. Lett.*, vol. 86, pp. 1–3, 2005.

[22] M. A. Noginov, G. Zhu, A. M. Belgrave, R. Bakker, V. M. Shalaev, E. E. Narimanov, S. Stout, E. Herz, T. Suteewong, and U. Wiesner, "Demonstration of a spaser-based nanolaser," *Nature*, vol. 460, pp. 1110–1113, 2009.

[23] J. Kottmann and O. Martin, "Plasmon resonant coupling in metallic nanowires," *Opt. Expr.*, vol. 8, pp. 655–663, 2001.

[24] P. Nordlander, C. Oubre, E. Prodan, K. Li, and M. Stockman, "Plasmon Hybridization in Nanoparticle Dimers," *Nano Lett.*, vol. 4, no. 5, pp. 899–903, 2004.

[25] B. Rolly, B. Stout, and N. Bonod, "Metallic dimers: When bonding transverse modes shine light," *Phys. Rev. B*, vol. 84, pp. 1–8, 2011.

[26] A. Devilez, B. Stout, and N. Bonod, "Mode-balancing far-field control of light localization in nanoantennas," *Phys. Rev. B*, vol. 81, pp. 1–5, 2010.

[27] N. K. Sakhnenko, N. P. Stognii, and A. Nerukh, "Hybridization of plasmons in coupled nanowires," in *Int. Conf. Micro- and Nano-photonics materail and devices*, Trento, Italy, 2012, pp. 69–72.

[28] N. Stognii and N. Sakhnenko, "Theoretical study of symmetric and antysymmetric plasmons in chains of coupled plasma cylinders," in *6th Eur. Conf. Antennas and Propagation*, Prague, Czech Republic, 2012, pp. 999–1002.

[29] D. M. Natarov, V. O. Byelobrov, R. Sauleau, T. M. Benson, and A. I. Nosich, "Periodicity—induced effects in the scattering and absorption of light by infinite and finite gratings of circular silver nanowires," *Opt. Expr.*, vol. 19, no. 22, pp. 22176–22190, 2011.

[30] E. I. Smotrova, A. I. Nosich, T. M. Benson, and P. Sewell, "Optical coupling of whispering-gallery modes of two identical microdisks and its effect on photonic molecule lasing," *IEEE J. Sel. Topics Quantum Electron.*, vol. 12, pp. 78–85, 2006.

[31] S. V. Boriskina, "Symmetry, degeneracy and optical confinement of modes in coupled microdisk resonators and photonic crystal cavities," *IEEE J. Sel. Topics Quantum Electron.*, vol. 12, no. 6, pp. 1175–1182, 2006.

[32] B. Rolly, N. Bonod, and B. Stout, "Dispersion relations in metal nanoparticle chains: Necessity of the multipole approach," *JOSA B*, vol. 29, no. 5, pp. 1012–1019, 2012.

Nadiia P. Stognii (S'11) was born in Kharkiv region, Ukraine, in 1987. She received the M.S. degree in mathematics from Kharkiv National Pedagogical University, Kharkiv, in 2010. She is currently toward working toward the Ph.D. degree in Department of Higher Mathematics, Kharkiv National University of Radio Electronics, Kharkiv.

Her research interests include plasmonics, mathematical modeling, differential and integral equations, frequency domain analysis, and analysis of wave interactions with transient plasma regions.

Ms. Stognii received the IEEE Antennas and Propagation Society Doctoral Award in the 2011. In 2012 she was supported under the German Academic Exchange Service (DAAD) grant for joint research with the University of Jena, Germany.

Nataliya K. Sakhnenko (M'02–SM'10) received the M.Sc. degree in mechanics and mathematics from the Kharkiv National University, Kharkiv, Ukraine, in 1992 and the Ph.D degree in radio physics from the Kharkiv National University of Radio Electronics, Kharkiv, Ukraine, in 2004.

She is an Associate Professor at Kharkiv National University of Radio Electronics. From 2004 to 2005 she held research fellowship from RS/NATO at G. Green Institute for Electromagnetics Research, the University of Nottingham, Nottinghamshire, U.K. From 2005 to 2008 she had NATO Reintegration Grant and grant from Ministry of Education and Science of Ukraine.Her current research interests include modeling of photonic, plasmonic, and metamaterial problems.

Plasmon Resonances and Their Quality Factors in a Finite Linear Chain of Coupled Metal Wires

Nadiia P. Stognii, *Student Member, IEEE*, and Nataliya K. Sakhnenko, *Senior Member, IEEE*

***Abstract*—This paper presents a straightforward analysis of the plasmonic properties of metal wires arranged in a linear chain of a finite length. For this we solve eigenvalue problem in form of matrix equations that allow thorough investigation of plasmonic modes with different field distributions. Our modeling provides results in terms of eigen oscillating frequencies and quality factors with controllable accuracy. It has revealed the possibility of quality factor dramatic enhancement for certain plasmonic modes by adjusting the separation distances and increasing the number of wires in a chain.**

***Index Terms*—Eigenvalues, nanowires, plasmons.**

I. Introduction

METALLIC nanostructures are the subject of immense interest in recent years due to the possibility of a strong light localization beyond the diffraction limit via the excitation of surface plasmons (SPs) [1], [2]. Various elements such as plasmonic waveguides [3], [4], subwavelength resonators [5], [6] and optical nanoantennas [7]–[9] have been studied recently. SPs have been explored for their potential in a single molecule detection [10], [11], biomolecular interaction studies [12], early stage cancer detection [13], [14], transmissions through the subwavelength apertures [15], [16], subwavelength imaging [17], etc.

Plasmonic structures of different shapes (nanowires, nanorods, nanospheres, and nanoshells) can be produced by various fabrication techniques. The silver nanowire structure is a candidate for key components in future ultracompact photonic devices [18]. It can be considered as a plasmon biosensor to monitor tiny biomolecular interactions [19] and as a novel modulator to control the intensity of the transmitted surface plasmon polaritons through a nanowire array [20]. Possible future nanophotonic technologies demand devices that can generate stimulated emission through the excitation of the SPs (spaser-based nanolaser). However, it is challenging problem due to the extremely strong absorption losses in metal at optical frequencies. The suggestion to compensate the losses by an optical gain using dye molecules in presence of metal nanoparticles [21] or using nanoparticles with gold core and dye-doped silica shell [22] has been tested in experiments recently. For these applications an accurate modeling that provides a valuable insight into fundamental phenomena is of great importance.

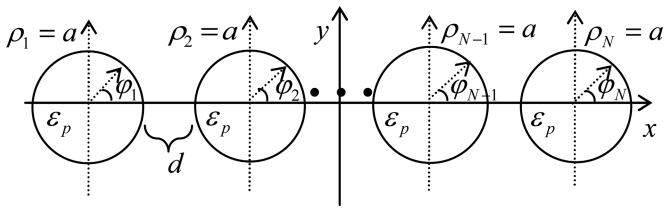

Fig. 1. Schematic diagram of the structure.

The plasmon resonances of nanoparticles with dimensions down to 2 nm can be investigated using classical Maxwell's theory [23], and their optical properties are characterized by their frequency dispersive complex permittivity. The resonance plasmon frequencies strongly depend on the particle size and shape. The plasmonic modes of coupled nanoobjects can be considered as symmetric and antisymmetric combinations of SPs of isolated objects with different frequencies and field portraits [24]–[28].

The plasmonic properties of nanowires and nanoparticles have recently been investigated using a variety of methods [4], [23]–[26], [32]. However, there is a lack of investigations in terms of quality Q factors of SPs, though these characteristics are of crucial importance in problems associated with spectral resolution of sensors, stimulated emission enhancement, etc. Many authors find SPs investigating resonance peaks in scattering cross section (SCS). This study cannot be considered as a complete one, because in this way only "bright" plasmons can be seen, "dark" plasmons that do not couple efficiently to incident wave cannot be discovered in such a description.

In this paper, we develop nonquasistatical expressions for the eigenvalues of SPs using the extension of the Drude formula to complex values that includes finding of eigenfrequencies and Q. Using this approach, all possible SPs can be found and investigated, including "dark" and multipole ones.

II. Mathematical Background

It is known that SPs can exist on a metal wire that can be considered as a plasma infinite-long cylinder (column) in the optical region. In this paper, we study the SP resonances in an isolated infinite-long wire and in a finite linear chain of coupled wires, surrounded by vacuum. The radius of each wire is a, the separation distance between them is d (air gap between the wires or interwires spacing), the time dependence $e^{i\omega t}$ is implied. Fig. 1 represents a schematic diagram of the structure. Cylinders with ordinary nonmagnetic metal are characterized by

Manuscript received August 1, 2012; revised January 1, 2013; accepted January 25, 2013. The work of the author N. Stognii was supported by the German Academic Exchange Service (DAAD). The work of the author N. K. Sakhnenko was supported by the European Science Foundation Research Networking Programme PLASMON-BIONANOSENSE.

The authors are with the Department of High Mathematics, Kharkiv National University of Radio Electronics, Kharkiv 61166, Ukraine (e-mail: nstognii@gmail.com; n_sakhnenko@yahoo.com).

Digital Object Identifier 10.1109/JSTQE.2013.2244561

a negative permittivity $\varepsilon < 0$ and support only TE polarized SPs. The frequency dependent metal's permittivity ε_p is described by the Drude model

$$\varepsilon_p = 1 - \omega_p^2/(\omega(\omega - i\gamma)) \tag{1}$$

where ω_p represents the plasma frequency and γ is the material absorption. We will assume that ω can be complex valued.

In this paper, the Maxwell equations are the underlying equations of the analysis

$$\text{rot}\,\vec{E} = -i\omega\mu_0\vec{H} \tag{2}$$

$$\text{rot}\,\vec{H} = i\omega\varepsilon_0\varepsilon\vec{E} \tag{3}$$

where $\vec{E}$ and $\vec{H}$ represent the vectors of electric and magnetic fields, ε_0 and μ_0 are the electric and magnetic constants, ε should be replaced by ε_p for inner points of wires, otherwise $\varepsilon = 1$.

To characterize the fields we introduce N cylindrical system of coordinates associated with each wire (see Fig. 1) and the global Cartesian (x, y, z) system centered at the midpoint of the structure. It is assumed that the columns are oriented along the axis *Oz*. *TE*-polarized fields are considered with H_z, E_φ, E_ρ nonzero components.

Maxwell's equations (2), (3) lead to the Helmholtz equation for the z-component of the magnetic field, which is denoted below as H

$$\Delta H + k^2 H = 0 \tag{4}$$

where $\Delta = \partial_{\rho\rho}^2 + 1/\rho\partial_\rho + 1/\rho^2\partial_{\varphi\varphi}^2$ is the Laplace operator, $k = \omega/c$ represents the wave number of vacuum, c is the light velocity in vacuum, for inner points of each wire $k = k_p$, and $k_p = n_p\omega/c$ is the wave number of plasma $n_p = \sqrt{\varepsilon_p(\omega)}$.

A. Isolated Infinite-long Metal Wire

We first investigate the SPs on isolated wire excited by a plane wave $H = e^{-ik(x\cos\alpha + y\sin\alpha)}$, here α is the angle between the direction of propagation of a plane wave and the positive direction of the x-axis (it is a z-component of the incident field, the normalizing factor is omitted). The transmitted and the scattered magnetic fields, respectively, are expanded as

$$H(\rho,\varphi) = \sum_{s=-\infty}^{+\infty} A_s J_s(k_p\rho)e^{is\varphi}, \quad \rho < a \tag{5}$$

$$H(\rho,\varphi) = \sum_{s=-\infty}^{+\infty} \bar{A}_s H_s^{(2)}(k\rho)e^{is\varphi}, \quad \rho > a \tag{6}$$

where A_s and $\bar{A}_s$ are unknown expansion coefficients. It should be noted that outside the wire the total field is the sum of incident plane wave and scattered field. The incident plane wave can be represented in the form of a series of the Bessel functions

$$e^{-ik(x\cos\alpha + y\sin\alpha)} = e^{-i\rho\cos(\varphi-\alpha)} = \sum_{s=-\infty}^{\infty} (-i)^s J_s(k\rho)e^{is(\varphi-\alpha)}. \tag{7}$$

The boundary conditions, that require the tangential components of the total electric and magnetic fields to be continuous at the surface, for this polarization can be written as follows:

$$H(\rho = a+0) = H(\rho = a-0) \tag{8}$$

$$\partial H/\partial\rho(\rho = a+0) = \varepsilon_p \cdot \partial H/\partial\rho(\rho = a-0). \tag{9}$$

Unknown coefficients are found by virtue of the substitution of (5), (6) and (7) into (8) and (9)

$$A_s = -(-i)^s e^{-is\alpha} n_p 2i/(\pi a)\cdot 1/F_s \tag{10}$$

$$\bar{A}_s = (-i)^s e^{-is\alpha}\cdot V_s/F_s \tag{11}$$

where

$$F_s = H_s^{(2)'}(ka)J_s(k_p a) - 1/n_p H_s^{(2)}(ka)J_s'(k_p a) \tag{12}$$

$$V_s = J_s'(ka)J_s(k_p a) - 1/n_p J_s(ka)J_s'(k_p a) \tag{13}$$

where the prime denotes the derivative with respect to the function's entire argument.

The plasmonic modes of the metal wire (the field in the absence of the incident field) can be written as

$$H = \begin{cases} AJ_s(k_p\rho)e^{is\varphi}, & \rho < a \\ \bar{A}H_s^{(2)}(k\rho)e^{is\varphi}, & \rho > a. \end{cases} \tag{14}$$

Similarly from the boundary conditions (8)–(9), one can obtain

$$A = \bar{A}H_s^{(2)}(ka)/J_s(k_p a) \tag{15}$$

and dispersion relation for eigenfrequencies of the wire

$$F_s = 0 \tag{16}$$

where F_s is given by (12). Equation (16) determines the eigenfrequencies of the isolated wire. We are interested in plasmonic modes, so we have to examine only the region $\omega < \omega_p$. In this interval (16) has no solution for the case $s = 0$, but for each integer positive s it has a unique plasmonic solution. SP with $s = 1$ can be considered as dipole SP, with $s = 2,\ 3, ...$ as multipole SPs.

B. Finite Linear Chain of Coupled Infinite-long Wires

The approach aforementioned can be extended to the case of N coupled metal wires arranged in a linear chain (see Fig. 1). For this, field representations which are similar to (5)–(6), have to be written for each wire

$$H(\rho_m,\varphi_m) = \sum_{s=-\infty}^{+\infty} A_s^m J_s(k_p\rho_m)e^{is\varphi_m}, \quad m = (1, ..., N) \tag{17}$$

$$H(\rho,\varphi) = \sum_{m=1}^{N}\sum_{s=-\infty}^{+\infty} \bar{A}_s^m H_s^{(2)}(k\rho_m)e^{is\varphi_m}. \tag{18}$$

Here, (17) presents internal field for each particular wire, while (18) characterizes external field, global polar coordinates (ρ, φ) are associated with the (x, y) Cartesian system. Unknown coefficients are found from the boundary conditions (8), (9) applied on each surface. Using the addition theorem for the Bessel functions we arrive at an infinite system of algebraic equations that can be truncated in order to provide a controlled numerical precision. The solution of the plane wave scattering problem on

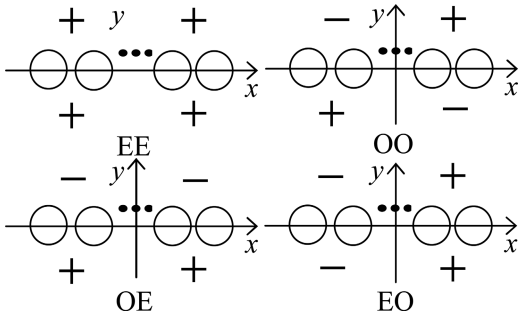

Fig. 2. Four classes of symmetry of the field: EE (x- even, y- even), OO (x- odd, y- odd), OE (x- odd, y- even), EO (x- even, y- odd).

a linear chain of silver nanowires is derived in [29]. In this paper, we concentrate on deriving the formulas for eigenfrequencies. For this we solve eigenvalue problem with zero incident field. Generally, the plasmonic eigenfrequencies of the linear chain are zeros of the N-block matrix determinant equation. With growing of N the solution of the equation becomes more time-consuming. However, the problem can be simplified using the following observations. The structure under consideration has two axes of symmetry, which causes four families of excited plasmons. They can be classified as EE SPs with field distributions symmetrical with respect to x- and y-axes, EO SPs with field distributions symmetrical (even) with respect to x-axis and antisymmetrical (odd) with respect to y-axis), similarly, OE (x-odd; y -even), OO (x-odd; y-odd). Here, we follow classification proposed in [30], [31] for eigenmodes in thin disks photonic molecules.

Fig. 2 shows the classification scheme of possible SP symmetry classes in a finite linear chain. For each symmetry class, the eigenfrequency equation can be simplified and written in the following form:

EE (x-even, y-even)

$$x_m^{(p)} + J_m(ka)\sum_{j=1}^{N/2}\sum_{s=0}^{\infty}\mu_s x_s^{(j)} U_s W_{m\,s}^{(p,j)} + \\ + 2J_m(ka)\sum_{s=0}^{\infty}\mu_s x_{2s}^{(N+1)/2} U_{2s} W_{m,2s}^{(p,(N+1)/2)} = 0 \quad (19)$$

OE (x-odd; y-even)

$$x_m^{(p)} - J_m(ka)\sum_{j=1}^{N/2}\sum_{s=1}^{\infty} x_s^{(j)} U_s W_{m\,s}^{(p,j)} + \\ + 2J_m(ka)\sum_{s=1}^{\infty} x_{2s}^{(N+1)/2} U_{2s} W_{m,2s}^{(p,(N+1)/2)} = 0 \quad (20)$$

EO (x-even; y-odd)

$$x_m^{(p)} - J_m(ka)\sum_{j=1}^{N/2}\sum_{s=0}^{\infty}\mu_s x_s^{(j)} U_s W_{m\,s}^{(p,j)} + \\ + 2J_m(ka)\sum_{s=0}^{\infty}\mu_s x_{2s}^{(N+1)/2} U_{2s} W_{m,2s}^{(p,(N+1)/2)} = 0 \quad (21)$$

OO (x-odd; y-odd)

$$x_m^{(p)} + J_m(ka)\sum_{j=1}^{N/2}\sum_{s=1}^{\infty} x_s^{(j)} U_s W_{m\,s}^{(p,j)} \\ + 2J_m(ka)\sum_{s=1}^{\infty} x_{2s}^{(N+1)/2} U_{2s} W_{m,2s}^{(p,(N+1)/2)} = 0 \quad (22)$$

where $m = (1, ...N)$, $p = (1, ...N/2)$ if N is even and $p = (1, ...(N+1)/2)$ if N is odd

$$x_m^{(p)} = A_m^{(p)} F_m J_m(ka)$$

$$U_{m\,s}^{(p,j)} = \frac{V_s}{F_s J_s(ka)}$$

$$W_{m\,s}^{(p,j)} = \begin{cases} \pm H_{m+s}^{(2)}((N-j)kh) \pm (-1)^s \\ \qquad H_{m-s}^{(2)}((N-j)kh), \quad p = j \\ H_{m-s}^{(2)}((j-p)kh) \pm (-1)^s H_{m+s}^{(2)}((j-p)kh) \\ +(-1)^s H_{m-s}^{(2)}((N-j)kh) \\ \qquad \pm H_{m+s}^{(2)}((N-j)kh), \quad p \neq j \end{cases}$$

$$W_{m\,s}^{(p,(N+1)/2)} = H_{m-2s}^{(2)}(((N+1)/2-p)kh) \\ \pm H_{m+2s}^{(2)}(((N+1)/2-p)kh)$$

$$h = 2a + d.$$

In $W_{m\,s}^{(p,j)}$ we take the sign $+$ for x-even SPs and $-$ for x-odd SPs. We have to stress that last terms in (19)–(22) appear only for odd number of columns in a chain.

Finding the eigenvalues reduces to the computation of zeros of the derived matrix equations determinants (19)–(22). These systems are the Fredholm second kind matrix equations. They can be truncated so that approximate solution will converge to exact solutions with increasing of the truncation number. The truncation number is determined by the wire radii the distance between them, and the desired accuracy. For accurate description of the fields, higher order multipole SPs should be taken into account for closely spaced wires. In this study, the truncation number 20 has been used to provide the 10^{-4} accuracy.

For distant wires due to decaying character of the Hankel functions the influence of the series terms become negligibly small. The derived equations can be viewed as characteristic equations for SP of isolated wire (16).

We have to mention that all eigenfrequencies are complex $\omega = \omega' + i\omega''$, where $\omega'' > 0$ represents damping and ω' is associated with the eigen oscillation frequencies. Q of plasmons can be evaluated through the formula $Q = \omega'/2\omega''$.

III. Results and Discussion

A. Plasmon Resonances of an Individual Metal Wire

For further calculations we will use the normalized parameter $w_p = \omega_p a c^{-1}$ that we will call the size parameter. Fig. 3 shows the spatial near-field portraits of the SPs for $s = 1,\ 2,\ 3$ ($w_p = 0.5$).

Fig. 4 plots the SCS obtained from (5), (6) in far-field limit versus normalized frequency (ka) for different values of

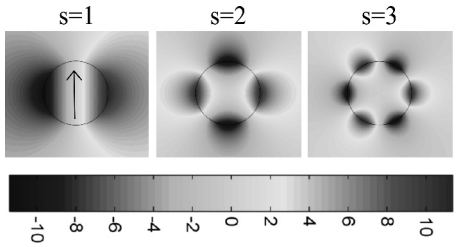

Fig. 3. Near-field distributions ($z-$ coordinate of the magnetic field) of SP for different number of angular field variations ($w_p = 0.5$).

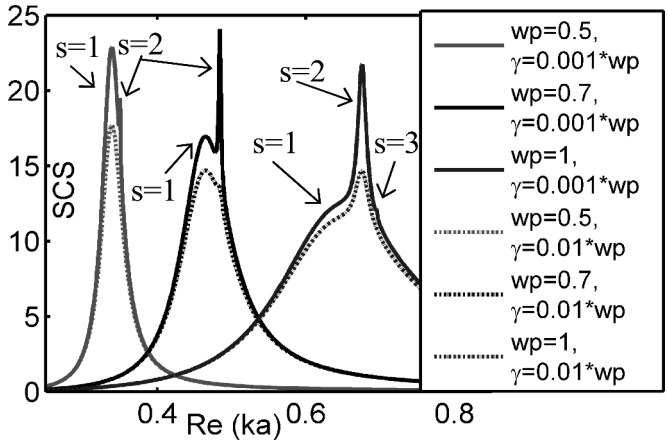

Fig. 4. SCS of isolated metal wire versus normalized frequency (ka) for different values of the size parameter w_p.

w_p. For the value of $w_p = 0.5$ (optically thin wire), we can see only one peak for $\gamma = 10^{-2} w_p$ associated with excited dipole plasmon. Additional sharp peak is observable in the spectrum for smaller value of losses $\gamma = 10^{-3} w_p$, it is associated with quadrupole plasmon. We see an additional prominent sharp peak for $w_p = 0.7$ if $\gamma = 10^{-3} w_p$ that corresponds to the quadrupole plasmon. For optically thick wire $(w_p = 1)$, maximum amplitude is associated with quadrupole SP. The normalized value of $w_p = 0.5$ approximately corresponds to the silver nanowire of 28.3 nm radius, $w_p = 0.7$ and $w_p = 1$ correspond to the 39.1 nm and 56.9 nm, respectively. Fig. 5(a) illustrates the value of the real part of SP normalized eigenfrequency $(\mathrm{Re}(ka) = \omega' a/c, \quad \omega'$ is the real part of eigenfrequency that is the solution of the equation (16)) versus the number of angular field variations (s) for the same values of the size parameters w_p as in Fig. 4. Fig. 5(b) plots Q of corresponding SPs. The dispersion (16) has formal solution for arbitrary number of angular field variations; different solutions for these values of w_p are observable only for a few SPs (dipole and quadrupole ones).

The SPs eigenvalues crowding is seen with growing of s (e.g. for $w_p = 1$ and $\gamma = 10^{-3} w_p$ dipole plasmon normalized eigenfrequency is $ka = 0.63 + 0.1i$, for quadrupole SP $ka = 0.6755 + 0.0068i$, with growing of s eigenfrequencies tend to the approximate value of $ka = 0.7 + 0.0005i$); however, in the spectrum (Fig. 4) only a dipole and quadrupole SPs are seen.

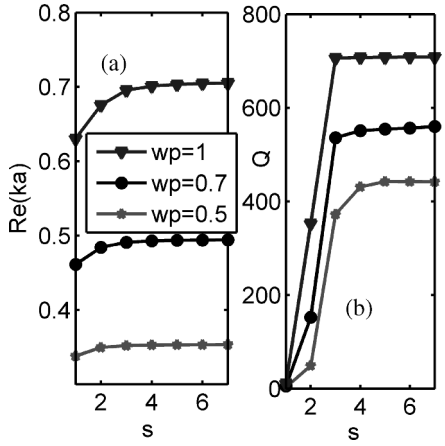

Fig. 5. (a) Dependence of the eigenfrequency on the number of angular field variations for different values of the w_p and (b) dependence of the Q-factor on the number of angular field variations for isolated plasma cylinder $(\gamma = w_p \cdot 5.10^{-3})$.

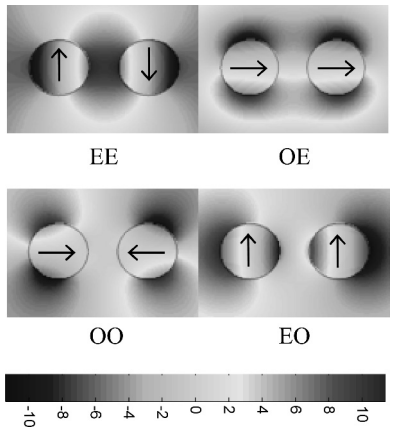

Fig. 6. Near-field distributions (z- coordinate of the magnetic field) of different SPs of two coupled metal wires ($w_p = 0.5$).

B. SPs of Two Coupled Wires

The SPs in dimmers have been extensively studied [23]–[25]. Here, we provide some additional comments in terms of eigenfrequencies and Q. Fig. 6 shows the near-field distributions (17), (18) of EE, EO, OE, OO dipole SPs (19)–(22) of two metal wires that are symmetric and asymmetric combinations of SPs of individual wire. The orientation of their dipole moments is shown in the figures. Dipole EE SP can be viewed as transverse opposite-phase plasmon. Dipole EO SP is transversal in-phase one, OE and OO are longitudinal SPs in-phase and opposite-phase, respectively.

Figs. 7 and 8 demonstrate the real values of the eigenfrequencies and Q for the dipole $(s = 1)$ and quadrupole $(s = 2)$ SPs for two coupled metal wires. Black dashed line plots data for an individual wire. It is clearly seen (see Fig. 7) that for distant wires eigenfrequencies are nearly identical for all four symmetry classes. As separation distance d becomes smaller, the frequency shift of the coupled SPs becomes much stronger.

Fig. 8 represents Q of coupled SP modes for dipole plasmon of optically thin wire $(w_p = 0.5)$ and quadrupole plasmon of thick wire $(w_p = 1)$. Dramatical enhancement of Q is observable

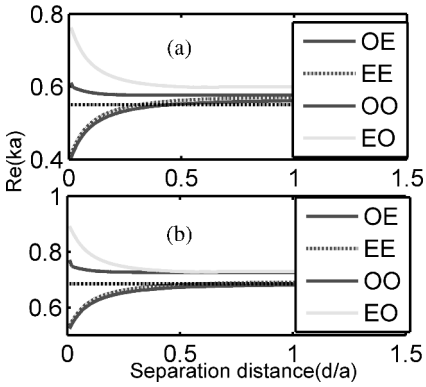

Fig. 7. Dependence of the normalized frequency on the normalized separation distance between two coupled wires for different SPs ($w_p = 1, \gamma = w_p \cdot 10^{-3}$): (a) $s = 1$; (b) $s = 2$.

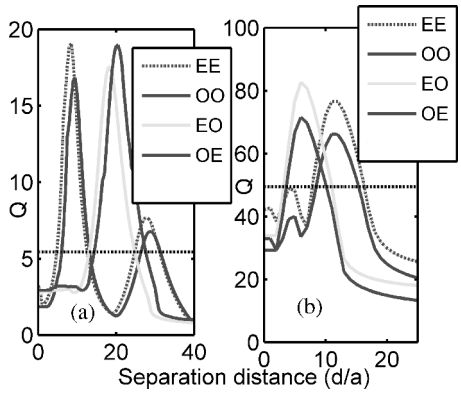

Fig. 8. Q-factor for two coupled metal wires ($\gamma = w_p \cdot 10^{-3}$) for EE, OE, EO, OO plasmons and for isolated wire for: (a) $w_p = 0.5$, s = 1; (b) $w_p = 1$, $s = 2$.

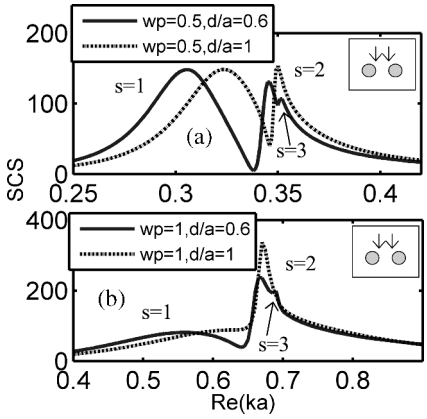

Fig. 9. SCS of a pair of metal wires versus normalized frequency (ka) for different values of the w_p and different values of the normalized separation distance ($\gamma = w_p \cdot 10^{-3}$). Illumination is along the normal to the main axis.

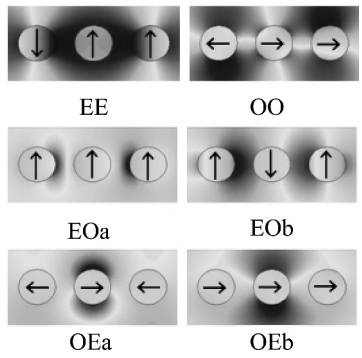

Fig. 10. Near-field distributions ($z-$ coordinate of the magnetic field) of different plasmons of three coupled metal wires.

when $d = 0.97\lambda$ for EE SP, $d = 1.86\lambda$ for EO SP, $d = 1.91\lambda$ for OE SP and $d = 1.025\lambda$ for OO SP (here λ is the wavelength) for thin wire dipole plasmons. Qs of coupled dipole SPs for these values of separation distances are evidently much greater than the Q of individual metal wire SP. For thick wires quadrupole SPs enhancement of Q is observable for following separation distances: $d = 1.43\lambda$ (EE), $d = 0.84\lambda$ (EO), $d = 0.82\lambda$ (OE) and $d = 1.41\lambda$ for OO SP.

In Fig. 9, we report SCS as a function of $\mathrm{Re}(ka)$ for two wires illuminated normally to their main axis. For this illumination direction only OE SPs are excited. It can be easily verified by comparing position of the peak in Fig. 9 and the value of ka in Fig. 7. For "thin" closely spaced wires ($w_p = 0.5, d/a = 0.6$, and $\gamma = w_p \cdot 10^{-3}$) only dipole and quadrupole modes are seen in the spectrum. Further, reduction of the separation distance leads to appearance of additional resonant peak ($s = 3$). With increasing of separation distance the spectrum becomes less complex with main peak at dipole plasmon and finally converges to that of a single wire (see Fig. 4). For thicker wires (lower panel, $w_p = 1$), we observe similar phenomena with main peak at quadrupole plasmon. For the illumination direction parallel to the main axis only EE SPs will be clearly seen in the spectrum, for this reason EE and OE plasmons are referred as "bright," while EO and OO as "dark" ones.

C. SPs of Three Coupled Nanowires

If we add one more metal wire, it would not alter the number of symmetry axes. However, additional solutions can appear in (19)–(22) that characterize bonding and antibonding combinations of the SPs. Thus, if the number of angular field variations is odd, bonding and antibonding SPs appear in EO and OE classes, while systems for EE and OO SPs possess unique solution for given s. However, for even s, we observe reverse situation that means appearance of bonding and antibonding modes in EE and OO classes. Fig. 10 demonstrates the near-field distributions of different dipole plasmons of three coupled wires. The orientation of their dipole moments is schematically shown in the figures. Here, OEb is longitudinal in-phase SP, OEa and OO are longitudinal opposite-phase SPs; EOa is transversal in-phase plasmon; EE and EOb are transversal opposite-phase ones.

Fig. 11 characterize the eigenfrequencies values (their real parts) of the all possible dipole and quadrupole plasmons in a chain of three coupled metal wires. It can be seen that the upward shift in frequency is much faster than downward shift for both dipole and quadrupole modes if wires are brought together. We compare the Q of dipole and quadrupole plasmons in a chain of three metal nanowires in Fig. 12. The growth of Q for certain separation distances is observable. Thus, the positions of Q maxima ($w_p = 0.5$) are: $d \approx 0.64\lambda$ (for EOb and OEb); $d \approx 0.84\lambda$

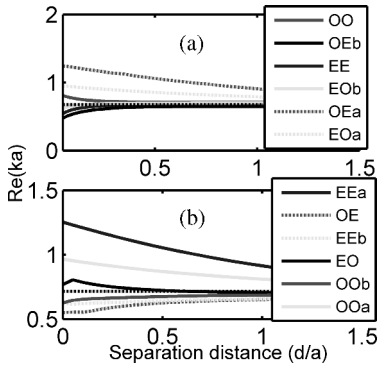

Fig. 11. Normalized frequency versus the normalized separation distance between the three coupled plasma cylinders and for isolated cylinder for different plasmons for $s = 1$ and $s = 2$ ($w_p = 1, \gamma = w_p \cdot 10^{-3}$).

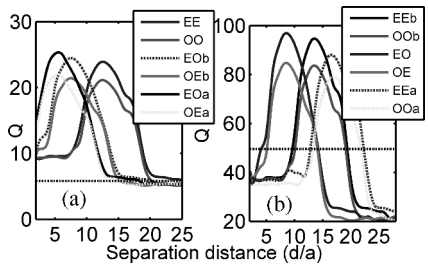

Fig. 12. Q-factor for three coupled plasma cylinders for ($\gamma = w_p \cdot 10^{-3}$) different SPPs for: (a) $w_p = 0.5$, $s = 1$; (b) $w_p = 1$, $s = 2$.

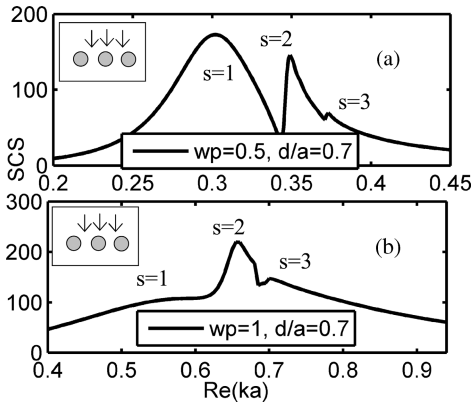

Fig. 13. SCS of three metal wires versus normalized frequency (*ka*) for different values of the w_p ($\gamma = w_p \cdot 10^{-3}$). Illumination is along the normal to the main axis.

(for EOa and OEa); and $d \approx 1.4\lambda$ (for OO and EE) [see Fig 12(a)]. For greater values of size parameter ($w_p = 1$) the results are presented for quadrupole plasmons [see Fig. 12(b)]. The increasing of Q is observable for $d \approx 0.8\lambda$ (for EO and OE); $d \approx 1.39\lambda$ (for EEa and OOa); and $d \approx 1.73\lambda$ (for EEb and OOb).

Fig. 13 represents the SCS of three metal wires chain with inter wires spacing $d \ll \lambda$. Similarly, to the two wires structure, multiple plasmons are seen in the spectrum. The distant peaks for strongly coupled wires would move closer with decreasing of the separation distance. Illuminating the chain from the top one excites longitudinal in-phase SP (OEb), $s = 2$ peak is associated with OE SP. For the illumination parallel to the main axis transversal opposite-phase EOb dipole plasmon can be excited. For three coupled wires these two dipole plasmons (OEb and EOb) are "bright" ones.

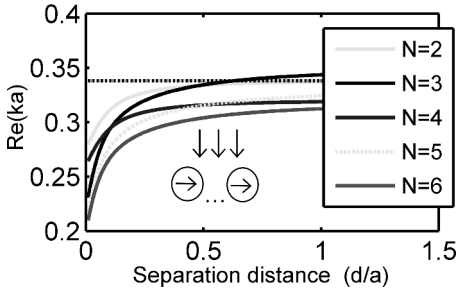

Fig. 14. Normalized frequency versus the normalized separation distance between the coupled metal wires in a chain on N columns for OE plasmon ($s = 1$, w_p =0.5, $\gamma = w_p \cdot 10^{-3}$) and for isolated wire ($s = 1$).

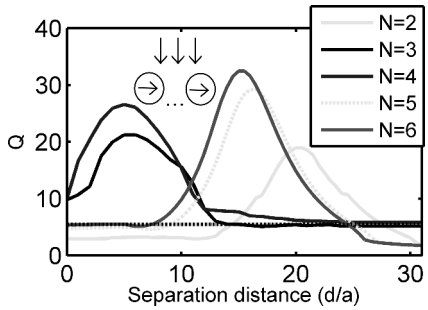

Fig. 15. Q-factor for chain of N coupled plasma cylinders ($s = 1$, $w_p = 0.5$, $y\gamma = w_p \cdot 10^{-3}$) for OE plasmons and for isolated cylinder.

D. P Resonances in a Linear Chain of Coupled Metal Wires

This approach can be extended to an arbitrary finite number of wires in a chain. Thus, in the case of four wires there exist eight SPs for each number of angular field variations, i.e., that each matrix (19)–(22) has two distinct solutions (bonding and antibonding SPs) for given value of s. In general, in the chain of N wires the total number of possible SPs for particular value of s equals to $2N$. In [29] there has been shown that additional resonances (grating-type ones) appear with growing of N (say $N < 50$).

Fig. 14 shows eigenfrequencies of bright dipole SPs for different number of wires in a chain. These SPs can be excited due to the Illumination normal to the major axis. The orientation of the dipole moments is shown in the inset in the figure. These SPs belong to the OE symmetry class. The horizontal line represents eigenfrequency of dipole plasmon of individual metal wire. Extra red shifting of coupled dipole plasmons at small separations is observable.

Enhancement of Q is seen for the same SP modes as aforementioned with appearance of each additional wire. The position of the peak depends on the number of wires; however, the maximum value of Q monotonically grows (see Fig. 15).

IV. Conclusion

We have systematically analyzed the plasmonic properties of a linear chain of metal wires within the Drude model. For this, we have derived matrix equations that allow thorough investigation of SPs. Our modeling provides results in terms of eigen oscillating frequencies and Q. It is shown that SP of coupled wires results from symmetric and antisymmetric combinations of the plasmons of individual wire and strongly depend on interwire separation. It has revealed the possibility of Q dramatic enhancement by virtue of placing the wires at certain distances and increasing the number of wires in a chain.

Acknowledgment

The authors are grateful to Prof. A. I. Nosich for many fruitful discussions.

References

[1] A. Zayats and I. Smolyaninov, "Near-field photonics: Surface plasmon polaritons and localized surface plasmons," *J. Opt. A, Pure Appl. Opt.*, vol. 5, pp. 16–50, 2003.

[2] W. Barnes, A. Dereux, and T. Ebbesen, "Surface plasmon subwavelength optics," *Nature*, vol. 424, pp. 824–830, 2003.

[3] S. Bozhevolnyi, V. Volkov, E. Devaux, J. Laluet, and T. Ebbesen, "Channel plasmon subwavelength waveguide components including interferometers and ring resonators," *Nature*, vol. 440, no. 7083, pp. 508–511, 2006.

[4] Y. Zhao and Y. Hao, "Finite-difference time-domain study of guided modes in nano-plasmonic waveguides," *IEEE Trans. Antennas Propag.*, vol. 55, pp. 3070–3077, 2007.

[5] H. R. Stuart and A. Pidwerbetsky, "Electrically small antenna elements using negative permittivity resonators," *IEEE Trans. Antennas Propag.*, vol. 54, pp. 1644–1653, 2006.

[6] J. li and N. Engheta, "Subwavelength plasmonic cavity resonator on a nanowire with periodic permittivity variation," *Phys. Rev. B*, vol. 74, pp. 1–11, 2006.

[7] P. Muhlschlegel, H. Eisler, O. Martin, B. Hecht, and D. Pohl, "Resonant optical antennas," *Science*, vol. 308, pp. 1607–1609, 2005.

[8] L. Novotny and N. Hulst, "Antennas for light," *Nature Photon.*, vol. 5, pp. 83–90, 2011.

[9] N. Bonod, A. Devilez, B. Rolly, S. Bidault, and B. Stout, "Ultracompact and unidirectional metallic antennas," *Phys. Rev. B*, vol. 82, pp. 1–6, 2010.

[10] K. Kneipp, Y. Wang, H. Kneipp, L. Perelman, I. Itzkan, R. Dasari, and M. Feld, "Single molecule detection using surface-enhanced Raman scattering (SERS)," *Phys. Rev. Lett.*, vol. 78, pp. 1667–1670, 1997.

[11] J. Bahns, A. Imre, V. Vlasko-Vlasov, J. Pearson, J. M. Hiller, L. H. Chen, and U. Welp, "Enhanced Raman scattering from focused surface plasmons," *Appl. Phys. Lett.*, vol. 91, pp. 1–3, 2007.

[12] J. Homola, "Surface plasmon resonance sensors for detection of chemical and biological species," *Chem. Rev.*, vol. 108, no. 2, pp. 462–493, 2008.

[13] S. Mallidi, T. Larson, J. Tam, P. Joshi, A. Karpiouk, K. Sokolov, and S. Emelianov, "Multiwavelength photoacoustic imaging and plamon resonance coupling of gold nanoparticles for selective detection of cancer," *Nano Lett*, vol. 9, no. 8, pp. 2825–2831, 2009.

[14] J. Kah, K. Kho, C. Lee, C. Richard, Sheppard, Z. Shen, K. Soo, and M. Olivo, "Early diagnostics of oral cancer based on the surface plasmon resonance of gold nanoparticles," *Int. J. Nanomedicine*, vol. 2, no. 4, pp. 785–798, 2007.

[15] J. Weiner, "The physics of light transmission through subwavelength apertures and aperture arrays," *Reports Progress Phys.*, vol. 72, pp. 1–19, 2009.

[16] T. Thio, K. Pellerin, R. Linke, H. Lezec, and T. Ebbesen, "Enhanced light transmission through a single subwavelength aperture," *Opt. Lett.*, vol. 26, pp. 1972–1974, 2001.

[17] I. Smolyaninov, J. Elliott, A. Zayats, and C. C. Davis, "Far-field optical microscopy with a nanometer-scale resolution based on the in-plane image magnification by Surface Plasmon Polaritons," *Phys. Rev. Lett.*, vol. 94, pp. 1–4, 2005.

[18] E. Ozbay, "Plasmonics: Merging photonics and electronics at nanoscale dimension," *Science*, vol. 311, pp. 189–193, 2006.

[19] K. Kim, S. J. Yoon, and D. Kim, "Nanowire-based enhancement of localized surface plasmon resonance for highly sensitive detection: A theoretical study," *Opt. Expr.*, vol. 14, no. 25, pp. 12419–12431, 2006.

[20] D. Fedyanin and A. Arsenin, "Transmission of surface plasmon polaritons through a nanowire array: Mechano-optical modulation and motion sensing," *Opt. Expr.*, vol. 18, no. 19, pp. 20115–20124, 2010.

[21] G. Dice, S. Mujumdar, and A. Elezzabi, "Plasmonically enhanced diffusive and subdiffusive metal nanoparticle-dye random laser," *Appl. Phys. Lett.*, vol. 86, pp. 1–3, 2005.

[22] M. A. Noginov, G. Zhu, A. M. Belgrave, R. Bakker, V. M. Shalaev, E. E. Narimanov, S. Stout, E. Herz, T. Suteewong, and U. Wiesner, "Demonstration of a spaser-based nanolaser," *Nature*, vol. 460, pp. 1110–1113, 2009.

[23] J. Kottmann and O. Martin, "Plasmon resonant coupling in metallic nanowires," *Opt. Expr.*, vol. 8, pp. 655–663, 2001.

[24] P. Nordlander, C. Oubre, E. Prodan, K. Li, and M. Stockman, "Plasmon Hybridization in Nanoparticle Dimers," *Nano Lett.*, vol. 4, no. 5, pp. 899–903, 2004.

[25] B. Rolly, B. Stout, and N. Bonod, "Metallic dimers: When bonding transverse modes shine light," *Phys. Rev. B*, vol. 84, pp. 1–8, 2011.

[26] A. Devilez, B. Stout, and N. Bonod, "Mode-balancing far-field control of light localization in nanoantennas," *Phys. Rev. B*, vol. 81, pp. 1–5, 2010.

[27] N. K. Sakhnenko, N. P. Stognii, and A. Nerukh, "Hybridization of plasmons in coupled nanowires," in *Int. Conf. Micro- and Nano-photonics materail and devices*, Trento, Italy, 2012, pp. 69–72.

[28] N. Stognii and N. Sakhnenko, "Theoretical study of symmetric and antysymmetric plasmons in chains of coupled plasma cylinders," in *6th Eur. Conf. Antennas and Propagation*, Prague, Czech Republic, 2012, pp. 999–1002.

[29] D. M. Natarov, V. O. Byelobrov, R. Sauleau, T. M. Benson, and A. I. Nosich, "Periodicity—induced effects in the scattering and absorption of light by infinite and finite gratings of circular silver nanowires," *Opt. Expr.*, vol. 19, no. 22, pp. 22176–22190, 2011.

[30] E. I. Smotrova, A. I. Nosich, T. M. Benson, and P. Sewell, "Optical coupling of whispering-gallery modes of two identical microdisks and its effect on photonic molecule lasing," *IEEE J. Sel. Topics Quantum Electron.*, vol. 12, pp. 78–85, 2006.

[31] S. V. Boriskina, "Symmetry, degeneracy and optical confinement of modes in coupled microdisk resonators and photonic crystal cavities," *IEEE J. Sel. Topics Quantum Electron.*, vol. 12, no. 6, pp. 1175–1182, 2006.

[32] B. Rolly, N. Bonod, and B. Stout, "Dispersion relations in metal nanoparticle chains: Necessity of the multipole approach," *JOSA B*, vol. 29, no. 5, pp. 1012–1019, 2012.

Nadiia P. Stognii (S'11) was born in Kharkiv region, Ukraine, in 1987. She received the M.S. degree in mathematics from Kharkiv National Pedagogical University, Kharkiv, in 2010. She is currently toward working toward the Ph.D. degree in Department of Higher Mathematics, Kharkiv National University of Radio Electronics, Kharkiv.

Her research interests include plasmonics, mathematical modeling, differential and integral equations, frequency domain analysis, and analysis of wave interactions with transient plasma regions.

Ms. Stognii received the IEEE Antennas and Propagation Society Doctoral Award in the 2011. In 2012 she was supported under the German Academic Exchange Service (DAAD) grant for joint research with the University of Jena, Germany.

Nataliya K. Sakhnenko (M'02–SM'10) received the M.Sc. degree in mechanics and mathematics from the Kharkiv National University, Kharkiv, Ukraine, in 1992 and the Ph.D degree in radio physics from the Kharkiv National University of Radio Electronics, Kharkiv, Ukraine, in 2004.

She is an Associate Professor at Kharkiv National University of Radio Electronics. From 2004 to 2005 she held research fellowship from RS/NATO at G. Green Institute for Electromagnetics Research, the University of Nottingham, Nottinghamshire, U.K. From 2005 to 2008 she had NATO Reintegration Grant and grant from Ministry of Education and Science of Ukraine.Her current research interests include modeling of photonic, plasmonic, and metamaterial problems.